Integrated optic frequency shifters for space heterodyne interferometry

Roman C. Gutierrez[a], Serge Dubovitsky[a] , Karl M. Kissa[b], Daniel J. Fritz[b]

[a]Jet Propulsion Laboratory, Pasadena, CA 91109
[b]Uniphase Telecommunications Products, Bloomfield, CN 06002

ABSTRACT

Heterodyne interferometer laser gauges are used in space-based astronomical interferometers to very accurately measure and compensate for variations in starlight pathlength. Bragg cells have been traditionally used to generate the heterodyne signal by shifting the frequency of the laser light. This paper presents the development and qualification of an integrated optic frequency shifter (IOFS) which offers improved performance and reliability compared with Bragg cell technology. The most critical advantage of the IOFS for space applications is that it enables fiber optic metrology source integration, which facilitates the integration process and results in more reliable and compact heterodyne interferometer laser gauges.

Keywords: acousto-optic tunable filter, frequency shifter, heterodyne interferometry

1. INTRODUCTION

Heterodyne interferometry uses two light beams of slightly different frequency which are combined on a photodetector to down-convert from optical frequency to the heterodyne frequency [1]. It is well known that the phase of the heterodyne signal is equal to the optical phase. By mixing down from optical frequency to a heterodyne frequency of 10 kHz to 100 kHz, the optical phase can be determined with sufficient accuracy for sub-nanometer metrology. For heterodyne interferometry to work, the two light beams must be coherent, so one typically uses a single optical source which is shifted in frequency by an acousto-optic device.

Leveraging from the development of the acousto-optic tunable filter (AOTF) for wavelength division multiplexing for fiberoptic telecommunications networks, we have designed, built, and tested a compact fiber pigtailed integrated optics frequency shifter (IOFS) for operation at 1.3 μm. We have measured conversion efficiencies exceeding 99% with an insertion loss of ~ 5 dB. These devices are rugged, small, and use low power RF electronics, making them ideal for use in space applications. The integrated optics approach for frequency shifters lends itself to the use of polarization maintaining fiber in metrology source system integration [2]. The use of fiber greatly improves the reliability aspects of the metrology source, since optical alignment issues are limited to the subsystem level. The use of fiber also reduces the overall weight and size of the metrology system which is important for space applications. It is the IOFS which makes fiberoptic integration possible.

In this paper, we describe in detail the operation of the IOFS and discuss issues for two possible approaches used to generate a 10 kHz to 100 kHz heterodyne signal. We describe the test setup used to characterize the IOFS and summarize the test results. To put these results in perspective, we compare with conventional Bragg cell technology. Comparing with the Bragg cell, the IOFS is a smaller, more robust device with lower power consumption, higher conversion efficiency, and comparable insertion loss.

2. DESCRIPTION

Acousto-optics describes the interaction between sound and light in any material. This interaction is a result of the change in optical index of refraction in a strained material, and it is called the photoelastic effect. An acoustic wave propagating through a crystal generates a strain wave, which in turn generates a moving index grating. As the light diffracts from the grating, it changes direction of propagation or polarization [3] such that the sum of the k vectors of the incident light and the acoustic wave equal the k vector of the diffracted light. Because the grating is moving, the frequency of the light is shifted. Another way to look at it is as the destruction of a photon and an acoustic phonon and the simultaneous generation of a photon which, because of energy conservation, has a frequency equal to the sum of the optical and acoustic frequencies.

The acousto-optic interaction in a bulk acousto-optic polarization converter [4] is illustrated in figure 1. In this configuration, the acoustic wave copropagates with a light beam perpendicular to the extraordinary axis of a uniaxial crystal. The input light is linearly polarized along the extraordinary axis. At the output of the crystal, the light is polarized along the ordinary axis and the frequency is shifted by the frequency of the acoustic wave. Because of phase matching requirements, good

conversion efficiency is only achieved for a small optical frequency range for a fixed acoustic frequency (and viceversa). The optical passband can be tuned by tuning the acoustic frequency. Because of this, this device was proposed as an acousto-optic tunable filter (AOTF).

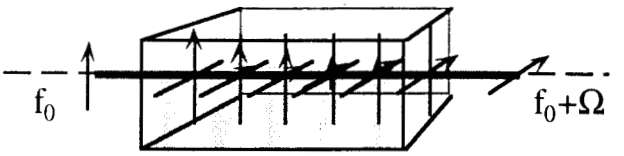

Figure 1. Schematic of a bulk acousto-optic polarization converter.

The integrated optics implementation of the AOTF [5] is shown in figure 2. The light is confined to a Titanium indiffussed waveguide where the index of the crystal is locally increased. Optical fiber is used to couple in and out of the Lithium Niobate chip. The piezoelectric effect of Lithium Niobate is used to excite the acoustic wave by using an interdigital surface acoustic wave (SAW) transducer. The acoustic wave is made to propagate along the optical waveguide where it interacts with the light. The interaction length is defined by two acoustic absorbers to achieve a high conversion efficiency. As for the bulk device, the integrated optics AOTF shifts both the frequency and polarization of the light. The frequency shift for these devices is around 210 MHz when used at an optical wavelength of 1.3 μm.

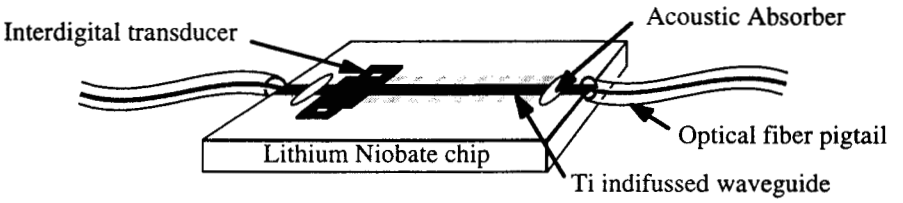

Figure 2. Schematic drawing of an integrated optics implementation of an AOTF.

To act as a band-pass filter, the device shown in figure 2 would have crossed polarizers at the input and output. Because these devices use Lithium Niobate optoelectronic chip technology, one proton exchanged polarizer with a polarization extinction ratio above 50 dB is integrated on chip. The crossed polarizer cannot be integrated on chip since the proton exchange process only yields polarizers in one axis. When used as a filter, the small change in frequency of the light is a side effect of little importance. Using the device in figure 2 as an IOFS, the filtering characteristics are a nuisance which requires that the Lithium Niobate chip be temperature controlled with a thermoelectric cooler.

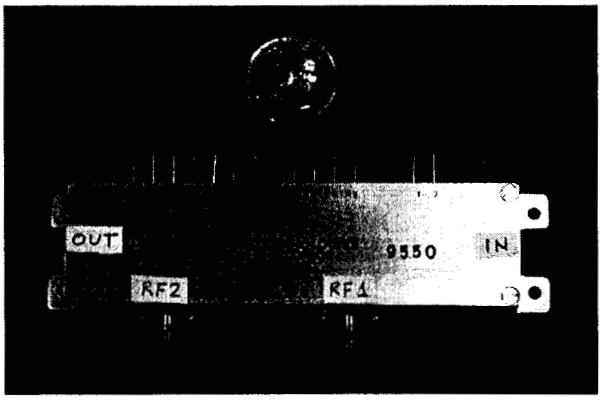

Figure 3. Picture of the integrated optics frequency shifter manufactured by UTP. Quarter shown for size comparison.

The IOFS we describe in this paper is manufactured by Uniphase Telecommunications Products. A picture of one such device is shown in figure 3. The device has two independent frequency shifters on one chip, so there are two optical fibers at the input and two fibers at the output. There are two SMA connectors for the RF signals that drive the SAW transducers. The

multiple single pin connectors on the top side of the IOFS are used for temperature control. There are two pins for thermo-electric cooler (TEC) contacts, two for the thermistor, and several other connectors for local heating of the chip.

3. ISSUES

For an ideal frequency shifter, all of the light is converted in frequency by Ω. Unfortunately, the integrated optic frequency shifter has a number of nonidealities which can place important limits on the resolution of a heterodyne metrology gauge. The actual operation of an IOFS is shown in figure 4. The output is composed of several sidebands as a result of polarization misalignment and imperfect conversion efficiency. The effect of these sidebands on an otherwise ideal heterodyne interferometer can be best looked using a mathematical treatment of heterodyne interferometry.

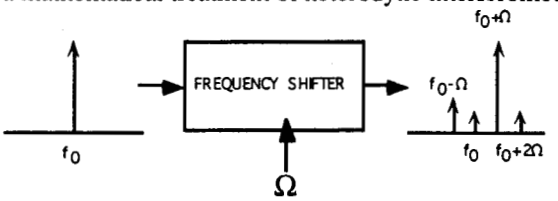

Figure 4. Diagram depicting actual operation of an IOFS.

In the coherent regime, we can treat the output of the frequency shifter as a sum of delta functions spaced apart by the frequency of the acoustic wave. Using this treatment, the complex field spectrum of the light coming out of an IOFS is given by:

$$S_1(\omega) = \sum_{n=-\infty}^{+\infty} a_n \delta(\omega - \omega_0 - n\Omega_1) \quad . \tag{1}$$

where Ω_1 is the frequency of the acoustic wave and ω_0 is the optical frequency. The coefficients in the summation are complex dimensionless constants that indicate the magnitude and phase of all sidebands. Because the frequency shift from a single IOFS is ~210 MHz, and a lower heterodyne frequency is usually required, a single frequency shifter cannot be used. One approach that is used to achieve a heterodyne frequency between 10 kHz and 100 kHz is to use of two IOFS's in parallel, as shown in figure 5. This configuration is referred to as the double frequency up-conversion.

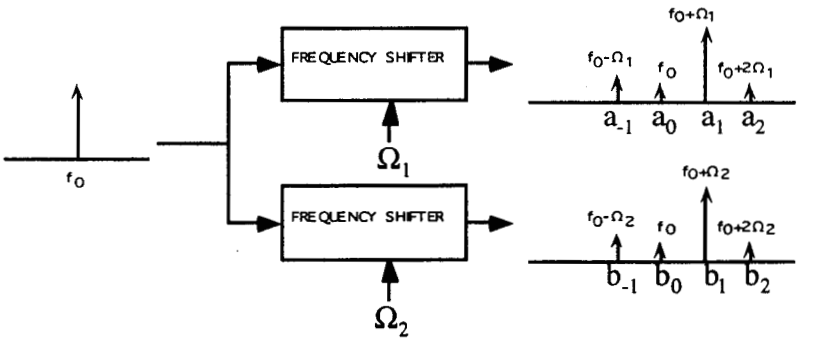

Figure 5. Double frequency up-conversion configuration to generate a heterodyne frequency between 10 kHz and 100 kHz using ~210 MHz frequency shifters.

Equation (1) describes the spectrum in one path of the interferometer, and the complex field spectrum of the light in the other path is given by a similar expression,

$$S_2(\omega) = \sum_{m=-\infty}^{+\infty} b_m \delta(\omega - \omega_0 - m\Omega_2) \, . \tag{2}$$

where Ω_2 is the frequency of the acoustic wave in the second IOFS.

The heterodyne interferometer combines the two light beams onto a photodetector where the intensity is measured. The intensity signal is then filtered by a demodulator at the heterodyne frequency $\Delta\Omega = \Omega_2 - \Omega_1$. It can be shown that the complex intensity function filtered at the modulation frequency is given by

$$I_{\Delta\Omega} = \sum_{n=-\infty}^{+\infty} \left(a_n^* b_{n+1} e^{i\frac{\omega_0 + (n+1)\Delta\Omega}{c}\Delta x} + b_n^* a_{n+1} e^{-i\frac{\omega_0 + n\Delta\Omega}{c}\Delta x} \right) \tag{3}$$

where Δx is the path delay between the reference and measurement paths. Using equation (3), the complex intensity function for a heterodyne interferometer using double frequency up-conversion is

$$I_{\Delta\Omega} = a_1 b_1 e^{i\phi} + a_{-1} b_{-1} e^{-i\phi} \tag{4}$$

where ϕ is the optical phase delay being measured by the interferometer. The first term in equation (4) is the desirable term. The second term in equation (4) is undesirable since it produces periodic nonlinear errors in the measurement of the optical phase. This is more clearly realized by looking at the mathematical expression for the phase that results from equation (4).

$$\phi_{measured} \approx \phi + \frac{a_{-1} b_{-1}}{a_1 b_1} \sin 2\phi \tag{5}$$

In equation (5), we have neglected higher frequency periodic nonlinearities which are of considerably lower magnitude. In figure 6, the negative sideband terms responsible for the nonlinearity are the only sideband terms that cause a problem.

A second approach to generate a heterodyne signal between 10 kHz and 100 kHz is the use of an up-down frequency shifter. This is an attractive implementation since it reduces insertion losses by half. A diagram illustrating this approach is shown in figure 6.

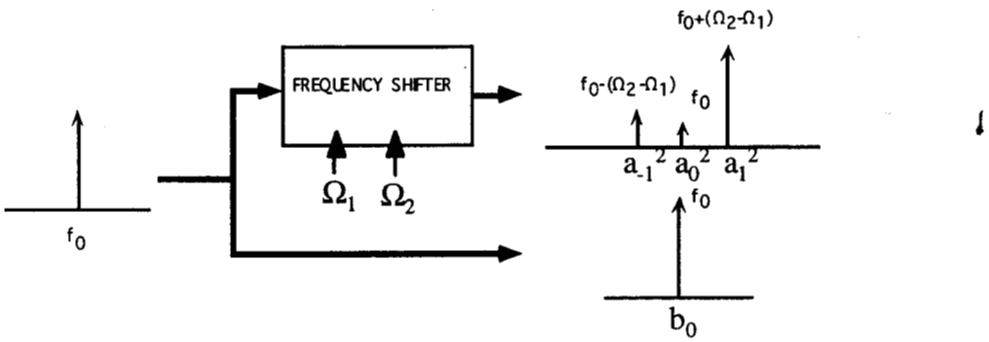

Figure 6. Up-down frequency shifter configuration to generate a heterodyne frequency between 10 kHz and 100 kHz using ~210 MHz frequency shifters.

Equation (3) is not valid for this calculation, but it can be shown that the complex intensity function filtered at the heterodyne frequency is given by

$$I_{\Delta\Omega} \approx a_1^2 b_0 e^{i\phi} + a_{-1}^2 b_0 e^{-i\phi} + a_0^2 a_1^2 \tag{6}$$

In equation (6), the additive term $a_0^2 a_{-1}^2$ is not included in the expression because it is negligible compared with the other terms in the equation.

Comparing equations (6) and (4), it is evident that the use of an up-down frequency shifter introduces an additional periodic nonlinearity term. The measured phase has a first harmonic periodic nonlinearity for the up-down frequency shifter, in addition to the second harmonic periodic nonlinearity which is present in either approach.

$$\phi_{measured} \approx \phi + \frac{a_0^2}{b_0} \sin\phi + \frac{a_{-1}^2}{a_1^2} \sin 2\phi \tag{7}$$

Equation (7) clearly shows that the unshifted light resulting from the imperfect conversion efficiency is an issue when using an up-down frequency shifter. Mathematically, unshifted light has the same effect as polarization leakage in the

interferometer optics. Polarization leakage is not an effect related to the frequency shifter; it is only referred to in this context since most people working in interferometry are acutely aware of the woes of polarization leakage. The "leakage" for the up-down frequency shifter can be reduced by using a polarizing section between the up-shifting and down-shifting stages. Without such a polarizer, the periodic nonlinearity may be too large even with 99% conversion efficiency. The double frequency up-conversion configuration, on the other hand, does not have any "leakage" and does not require the extra polarizer.

4. TEST SETUP

The IOFS from Uniphase Telecommunications Products have been extensively tested both at JPL and at UTP. Figure 7 shows the test setup used to characterize the devices at JPL. This automated test setup was developed at JPL to enable insitu testing of the devices during environmental testing, which is planned for the near future.

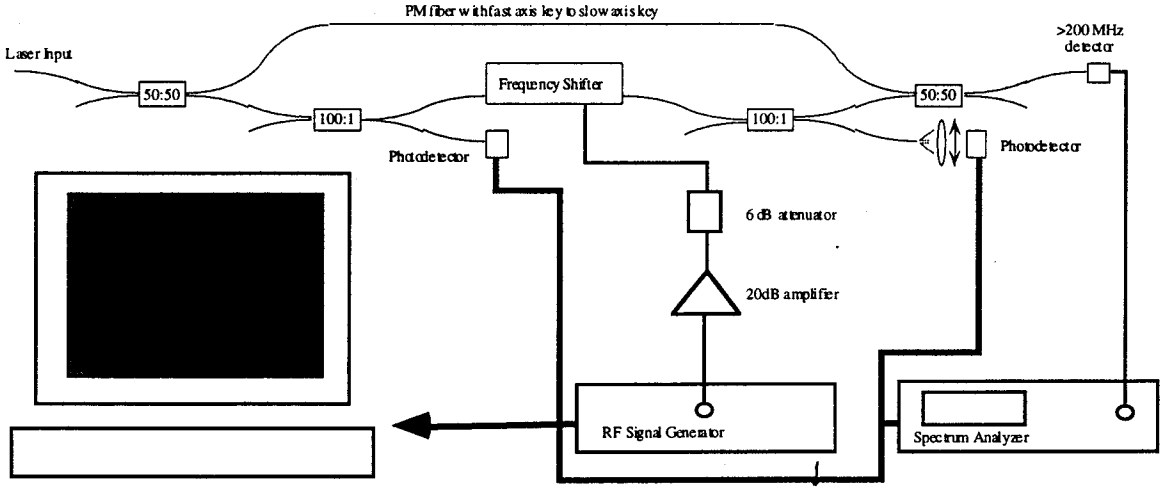

Figure 7. Diagram of the JPL IOFS automated test setup.

Light at 1.3 μm from a Nd:YAG laser is coupled into PM fiber. PM fiber couplers from Canadian Instrumentation and Research are used to monitor the input and output of the IOFS. A reference fiber is used to beat the frequency shifted light with the unshifted light on a fast detector.

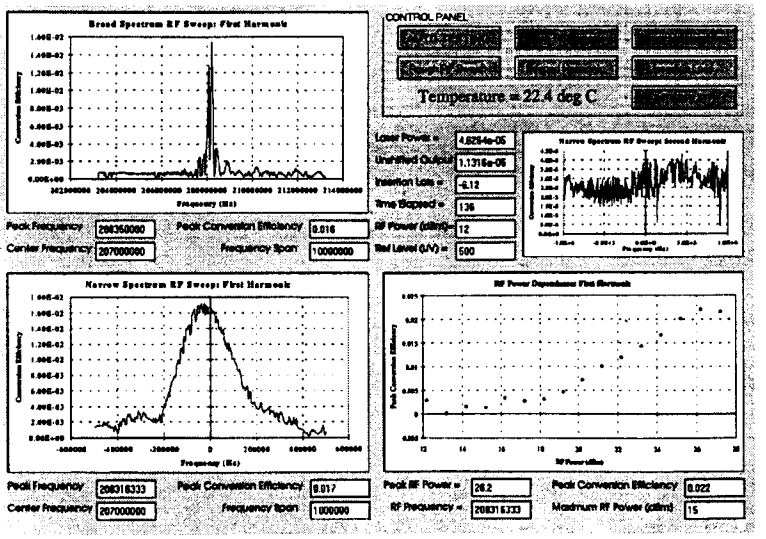

Figure 8. Automated test setup software written in Microsoft Visual Basic.

The output photodetector has a polarizer in front of it to be able to measure both insertion loss and conversion efficiency. The polarizer is set such that the output is maximized when the IOFS is inactive. With the IOFS off, the insertion loss is

measured. When the IOFS is turned on, the output polarization is orthogonal to the polarizer, and the power detected on the photodetector is decreased. The conversion efficiency is determined by comparing the photodetector output with the IOFS on and off. The conversion efficiency is monitored continuously by looking at the magnitude of the beat signal on the fast detector when the IOFS is turned on. As the frequency of the RF signal input to the IOFS is changed, we trace the conversion efficiency as a function of RF frequency using the fact detector output and the spectrum analyzer. The conversion efficiency is recorded at a single RF frequency and several values of the RF power to optimize all settings for the RF generator. To quantify the magnitude of the negative sideband (which is responsible for periodic nonlinearities as described in the previous section), the reference fiber is disconnected, and the signal at twice the RF frequency is measured as a function of the RF frequency. To measure the second positive sideband (not really required), the reference fiber is reconnected, and the measurement is repeated.

The computer screen for the automated test setup software is shown in figure 8. The data in the figure is not representative of these devices (it is for a 1.5 μm device operated at 1.3 μm), but it shows that all the necessary data is automatically generated using the "AUTO TESTING" button in the control panel. The approximate duration of the whole test is 5 minutes. This software, which controls the photodetectors, an RF signal generator and a spectrum analyzer through GPIB commands, was written using Microsoft Visual Basic.

5. TEST RESULTS

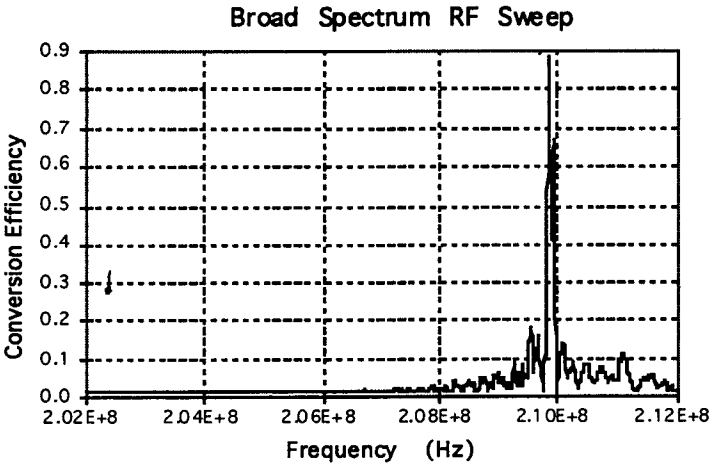

Figure 9a. Conversion efficiency as a function of RF frequency for UTP #3181-3B RF2. Peak conversion efficiency can be seen around 210 MHz.

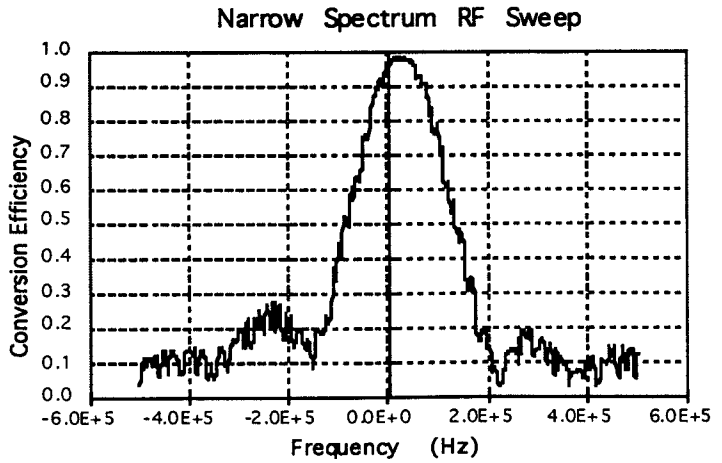

Figure 9b. Conversion efficiency as a function of RF frequency around peak for UTP #3181-3B RF2. Passband for the IOFS is about 100 kHz.

The tests results for device UTP #3181-3B RF2, which are representative of all IOFS devices, are shown in figure 9. The broad spectrum RF sweep is used to pinpoint the RF frequency for peak conversion efficiency. The measurement shown in figure 9a was taken at room temperature. The data shows that the optimum RF frequency is around 210 MHz. The narrow spectrum RF sweep shown in figure 9b shows the conversion efficiency as a function of RF frequency in a range of 1 MHz around the peak frequency as estimated from the broad spectrum RF sweep. This data is used to extract a more accurate value for the optimum RF frequency and also determines the operating bandwidth. In this case, the 3 dB bandwidth is about 200 kHz. The bandwidth determines the requirements on temperature stability since the peak conversion efficiency changes frequency with temperature at about 100 kHz/°C.

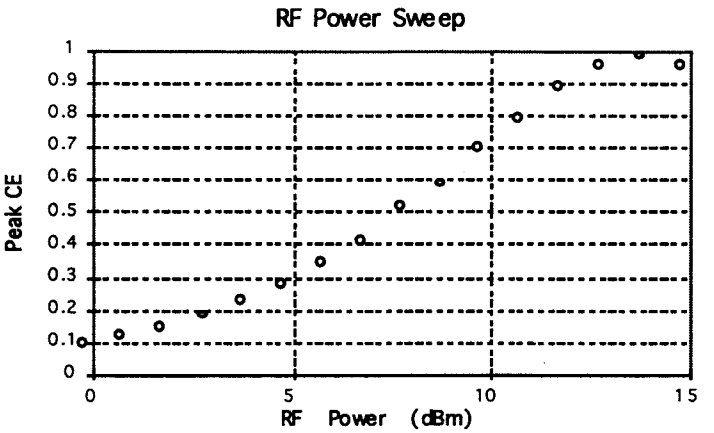

Figure 9c. Peak conversion efficiency as a function of RF power for UTP #3181-3B RF2. Optimum RF power is ~14 dBm. Maximum conversion efficiency is ~99%.

Figure 9c shows the conversion efficiency at the optimum RF as a function of the RF power. Initially, as the RF power is increased, the conversion efficiency increases. After the optimum value of 14 dBm, any further increase in RF power actually decreases the conversion efficiency at the optimum RF power. It is not known if the decrease for higher RF power may be due in part to heating of the crystal changing the optimum RF frequency. Figure 9d shows the measurement on the fast photodetector at twice the RF frequency as it is swept across the narrow RF spectrum sweep. It shows that there is definitely a signal present. In this case, it indicates a negative sideband intensity of -38 dBc. The measurements made at UTP indicate a much smaller value for this same device, so these measurements will have to be repeated in the future to verify this very important piece of data. At -40 dBc, an otherwise ideal heterodyne interferometer would have a periodic nonlinearity of about 0.1 nanometer. At -60 dBc, the nonlinearity drops to about 1 picometer.

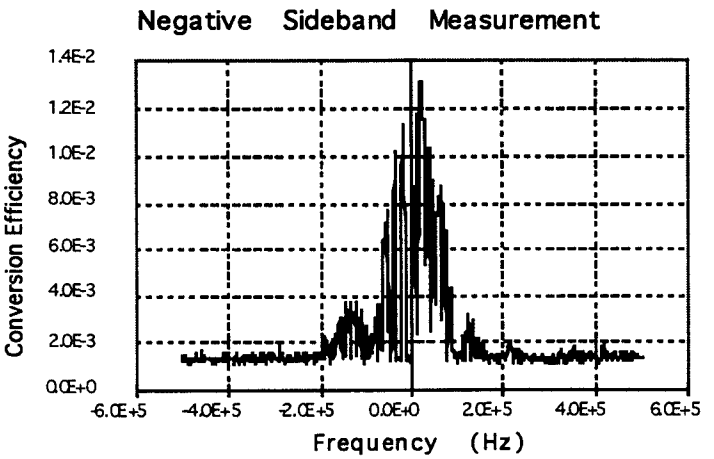

Figure 9d. Second harmonic measurements for UTP #3181-3B RF2. Negative sideband is about -38dBc.

A summary of the data gathered on four IOFS's from UTP is shown in Table 1. On two of these frequency shifters, the optimum RF power is 26 dBm instead of 14 dBm. This is because a wire was used inside the package to route the RF signal

to the SAW transducer, and the impedance of the line was not properly matched. For future devices, power requirement should be 14 dBm for all devices. The most recent device we tested is not shown in this table, but is worthwhile mentioning because of the improvements in the insertion loss. The insertion loss for this new device is about 3 dB, possibly due to improvements in the pigtailing. All other parameters remained nearly the same.

In order to put the results described in this section in perspective, we can compare these results with the specifications from commercially available Bragg cells. Bragg cells are the most common frequency shifters used for heterodyne interferometry. Typical conversion efficiency for a Bragg cell is around 85 %, which is lower than for the IOFS which can be greater than 99%. The RF power required to drive a sound wave in a bulk crystal is much higher than the power required by a SAW transducer. Typically, Bragg cells require at least 30 dBm of RF power, compared with 14 dBm for the IOFS. Because the Bragg cell is a bulk optic device, in order to have fiber pigtails, careful optical alignments between collimating lenses and fibers are required to achieve a low insertion loss. If the alignments are properly made, Bragg cells have comparable insertion loss to the IOFS. But the fact that it is so sensitive to bulk optics alignments makes the Bragg cell a less robust frequency shifter. Because of the trouble with "pigtailing" Bragg cells, they are usually used as bulk optic components. Metrology source integration is then done on an optical bench to stabilize the optical alignment between the different components making up the metrology source. Using IOFS, the metrology source integration is done using optical fiber, yieling a lighter more robust architecture that is more amenable for use in space.

#20407 RF1

	JPL Results	UTP Results
Peak RF Freq	209.93 MHz	210 MHz
Peak RF Power	14 dBm	13 dBm
Peak Con. Eff.	97 %	96 %
Insertion Loss	6.52 dB	5.87 dB
Output PER	35 dB	34 dB
Neg. SideB	-52 dBc	-70 dBc
T. Scale Fac.	–	110 kHz/°C

#3181-3B RF1

	JPL Results	UTP Results
Peak RF Freq	209.85 MHz	210 MHz
Peak RF Power	14 dBm	–
Peak Con. Eff.	99 %	99 %
Insertion Loss	4 dB	–
Output PER	33.1 dB	32 dB
Neg. Side B.	-36 dBc	-60 dBc
T. Scale Fac.		110 kHz/°C

#20407 RF2

	JPL Results	UTP Results
Peak RF Freq	210.02 MHz	210 MHz
Peak RF Power	26 dBm	24 dBm
Peak Con. Eff.	96 %	96 %
Insertion Loss	7.01 dB	5.82 dB
Output PER	29.6 dB	33 dB
Neg. Side B.	-54 dBc	-60 dBc
T. Scale Fac.	–	110 kHz/°C

#3181-3B RF2

	JPL Results	UTP Results
Peak RF Freq	209.86 MHz	210 MHz
Peak RF Power	24 dBm	–
Peak Con. Eff.	99 %	99 %
Insertion Loss	4.62 dB	–
Output PER	32.9 dB	32 dB
Neg. Side B.	-38 dBc	-56 dBc
T. Scale Fac.		110 kHz/°C

Table 1. Summary of IOFS data from JPL and UTP.

6. CONCLUSION

This paper describes a commercially available technology that is usable as a frequency shifter for heterodyne interferometry. UTP has manufactured several IOFS, and these have been evaluated both at JPL and at UTP. The test results show that IOFS's operating at 1.3 μm have measured conversion efficiency exceeding 99% and an insertion loss as low as 3 dB. These devices are rugged, small, and use low power RF electronics, making them ideal for use in space applications. These devices were originally developed as filters for wavelength division multiplexing for fiber optic communications, but they make excellent frequency shifters for heterodyne interferometry.

We have discussed two possible approaches used to generate a 10 kHz to 100 kHz heterodyne signal using the 210 MHz frequency shift of an IOFS. It is concluded that one of these approaches generates less periodic nonlinearities on an otherwise ideal heterodyne interferometer. We described the test setup used to characterize the IOFS and summarized the test results. Comparing with the Bragg cell, which is the technology typically used as a frequency shifter in heterodyne interferometry, the IOFS is a smaller, more robust device with lower power consumption, and higher conversion efficiency. Most importantly,

the IOFS simplifies the integration of a metrology source by making optical fiber integration possible. An all-fiber integration makes the metrology source more robust and light weight and simplifies the distribution of the optical signals to the interferometers.

This work was performed at the Jet Propulsion Laboratory, California Institute of Technology under a contract with the National Aeronautics and Space Administration.

7. REFERENCES

1. R. Crane, "Interference phase measurement", *Appl. Opt.*, Vol. 8, No. 3, pp. 538-542, 1969.
2. S. Dubovitsky, D. Seidel, D. Liu, and R. Gutierrez, "Metrology source for high-resolution heterodyne interferometer laser gauges", in SPIE Astronomical Interferometry, Kona, Hawaii, paper 3350-50, 1998.
3. R.W. Dixon, "Acoustic Diffraction of Light in Anisotropic Media", *IEEE J. Quantum Elec.*, Vol. QE-3, No. 2, pp. 85-93, 1967.
4. S.E. Harris and R.W. Wallace, "Acousto-Optic Tunable Filter", *J. Opt. Soc. Amer.*, Vol. 59, No. 6, pp. 744-747, 1969.
5. David Smith, Jane E. Baran, John J. Johnson, and Kwok-wai Cheung, "Integrated-Optic Acoustically-Tunable Filters for WDM Networks", *IEEE J. Sel. Areas Comm.*, Vol. 8, No. 6, pp. 1151-1159, 1990.